Available online at www.sciencedirect.com
ScienceDirect
Biochimica et Biophysica Acta XX-XX
BIOCHIMICA ET BIOPHYSICA ACTA
BBA
www.elsevier.com/locate/bbamcr

Cytoplasmic Ca^{2+} signals and cellular death by apoptosis in myocardiac H9c2 cells

Antonio Lax, Fernando Soler, Francisco Fernández-Belda *

Departamento de Bioquímica y Biología Molecular A, Edificio de Veterinaria, Universidad de Murcia, Campus de Espinardo, 30071 Murcia, Spain

Received 15 February 2006; received in revised form 4 May 2006; accepted 12 May 2006
Available online cc

Abstract

The incubation of H9c2 cells with 10 μM thapsigargin (TG) was associated with the appearance of a two-component cytoplasmic Ca^{2+} peak. Experiments performed in a Ca^{2+}-free medium indicated that both components came from intracellular sources. The first component of the signal corresponded to the discharge of the sarco-endoplasmic reticulum (SER) Ca^{2+} store. The appearance of the second component was prevented by cell preincubation with cyclosporin A (CsA) and gave rise to a clear and permanent depolarization of the mitochondrial inner membrane. These features were indication of a mitochondrial origin. The observed release of mitochondrial Ca^{2+} was related with opening of the permeability transition pore (PTP). The two-component cytoplasmic Ca^{2+} peak, i.e., treatment with 10 μM TG, as compared with the first component alone, i.e., treatment with 3 μM TG, was associated with a faster process of cellular death. In both cases, chromatin fragmentation and condensation at the nuclear periphery were observed. Other prominent apoptotic events such as loss of DNA content and cleavage of poly(ADP-ribose) polymerase (PARP) were also dependent on TG concentration and occurred in different time windows. PTP opening induced by 10 μM TG was responsible for the faster apoptotic death.

Keywords: Ca^{2+} signal; Thapsigargin; Sarco-endoplasmic reticulum; Permeability transition pore; Apoptosis; Cardiac cell line

1. Introduction

Cytoplasmic Ca^{2+} elevations are used as intracellular signals to activate a wide variety of cellular processes [1]. The versatility of this apparently simple regulatory mechanism relies in the existence of local Ca^{2+} events [2,3]. The so-called elementary Ca^{2+} signals, generated by the coordinated opening of Ca^{2+}-channel clusters, are responsible for the activation of specific processes at discrete cellular locations. Moreover, the elementary Ca^{2+} signals can be recruited in different ways to create global Ca^{2+} signals [4]. Global Ca^{2+} signals can even pass between coupled cells to coordinate the activities of whole tissues or organs [5,6].

Intracellular Ca^{2+} signals are usually delivered as brief Ca^{2+} rises. In some cases, a single Ca^{2+} spike is sufficient to trigger a cellular response. However, when a longer Ca^{2+} signal is necessary the spikes are repeated in the form of Ca^{2+} waves [7]. The resting Ca^{2+} level also encodes information, thus a low amplitude but sustained increase in cytoplasmic Ca^{2+} induces activation of the nuclear factor of activated T cells or NFAT [8]. The calcineurin/NFAT pathway has been implicated in a transgenic model of pathological cardiac hypertrophy [9]. Besides, a large and sustained elevation of cytoplasmic Ca^{2+} as that occurring in myocardial ischemia [10] is considered a death signal giving rise "in vitro" to the apoptotic program [11,12]. Apoptosis of cardiomyocytes has been consistently observed in experimental models of cardiac diseases [13–16].

Ca^{2+} signaling in cardiac myocytes constitutes a striking model since multiple Ca^{2+} signals coexist with repetitive

Abbreviations: SER, sarco-endoplasmic reticulum; EGTA, ethylene glycol-bis(β-aminoethyl ether)-*N,N,N′,N′*-tetraacetic acid; HEPES, 4-(2-hydroxyethyl) piperazine-1-ethanesulfonic acid; BHQ, 2,5-di(*t*-butyl)hydroquinone; TG, thapsigargin; TMRM, tetramethylrhodamine methyl ester; ECM, extracellular medium; DMEM, Dulbecco's modified Eagle's medium; PBS, phosphate-buffered saline; IO, ionomycin; $\Delta\Psi_m$, mitochondrial inner membrane potential; CsA, cyclosporin A; PTP, permeability transition pore; MTT, 3-(4,5-dimethylthiazol-2-yl)-2,5-diphenyltetrazolium bromide; AO, acridine orange; PI, propidium iodide; PARP, poly(ADP-ribose) polymerase

* Corresponding author. Tel.: +34 968 364 763; fax: +34 968 364 147.
E-mail address: fbelda@um.es (F. Fernández-Belda).

0167-4889/$ - see front matter

cytoplasmic Ca^{2+} spikes that are involved in the generation of each heart beat. In this context, the role of altered Ca^{2+} signals as a critical parameter in cardiac myocytes apoptosis is an interesting research subject deserving attention.

The SER is the main intracellular Ca^{2+} store playing a key role in Ca^{2+} signaling. There is also mounting evidence that the mitochondrion is involved in Ca^{2+} regulation due to the ability of this organelle to store and release Ca^{2+} [11]. Ca^{2+} signals arising from the SER are mediated by activation of either the ryanodine or the inositol trisphosphate receptor whereas the recovery of the resting Ca^{2+} level occurs via the SER-resident Ca^{2+}-ATPase. Therefore, the alteration of any of these transport systems leads to disruption of the cytoplasmic Ca^{2+} homeostasis.

Early studies indicated that a rapid and dose-dependent increase in cytoplasmic Ca^{2+} is the common cellular response after addition of TG and this was observed in the absence of extracellular Ca^{2+} [17,18]. The experimental evidence also confirmed that SER Ca^{2+}-ATPase is the TG target in cardiac muscle cells [19]. The link between TG-induced cytoplasmic Ca^{2+} rise and activation of apoptosis has been reported in different cell types [20–22], even though the underlying mechanism is not fully understood.

The present study deals with characterization of intracellular Ca^{2+} pools that are sensitive to TG and the involvement of different Ca^{2+} signals induced by TG on cellular death by apoptosis. This was approached by using the cardiac cell line H9c2 as a model system and measuring Ca^{2+} fluxes and the tetramethylrhodamine methyl ester (TMRM) response in different experimental setting. Some morphological and functional parameters related with specific mechanisms of cellular demise were also evaluated.

2. Materials and methods

2.1. Reagents and materials

TG, 2,5-di(*t*-butyl)hydroquinone (BHQ), ionomycin (IO), CsA from *Tolypocladium inflatum*, 3-(4,5-dimethylthiazol-2-yl)-2,5-diphenyltetrazolium bromide (MTT), acridine orange (AO), propidium iodide (PI) and other analytical reagents were obtained from Sigma. Acetoxymethyl derivatives of Fura-2, Rhod-2 and Fluo-4, as well as TMRM and Pluronic® F-127, were from Molecular Probes Europe. Stock solutions of Ca^{2+} probes were prepared in anhydrous dimethyl sulfoxide. Culture reagents including low glucose Dulbecco's modified Eagle's medium (DMEM) with L-glutamine, fetal bovine serum, penicillin-streptomycin-L-glutamine solution and the trypsinization medium containing 0.25% trypsin were from Gibco. The $CaCl_2$ standard solution Titrisol® was purchased from Merck. The rabbit anti-human PARP polyclonal antibody (H-250) was from Santa Cruz Biotechnology. Mouse monoclonal anti-γ-tubulin (clone GTU-88), peroxidase-conjugated goat anti-rabbit IgG (whole molecule), peroxidase-conjugated rabbit anti-mouse IgG (whole molecule), Chemichrome Western Control (C 4236), Chemiluminescent Peroxidase Substrate (CPS-1) and Protease Inhibitor Cocktail (P 8340) were from Sigma. Protran® BA 83 nitrocellulose transfer membrane was provided by Schleicher and Schuell BioScience. Qentix™ Western Blot Signal Enhancer was from Pierce and Curix, RP2 plus film was from Agfa.

2.2. Cell culture

The H9c2 cell line derived from embryonic rat heart was obtained from the European Collection of Cell Cultures (www.ecacc.org.uk). Low passage cells were maintained at 37 °C in a humidified atmosphere with 95% air and 5% CO_2 using standard culture procedures. They were split or harvested when ~70% confluence was reached. The culture medium was DMEM supplemented with 10% heat-inactivated fetal bovine serum, 2 mM L-glutamine, 100 units/ml penicillin and 100 μg/ml streptomycin [23]. All the studies were conducted in the absence of fetal bovine serum and antibiotics. When the TG treatment was prolonged for hours or days the apoptotic effect of serum deprivation was corrected by running control experiments in the absence of TG. When indicated cells were incubated/diluted in extracellular medium (ECM) with Ca^{2+} composed of 10 mM 4-(2-hydroxyethyl)piperazine-1-ethanesulfonic acid (HEPES)-NaOH, 121 mM NaCl, 4.7 mM KCl, 1 mM $CaCl_2$, 1.2 mM $MgSO_4$, 5 mM $NaHCO_3$, 1.2 mM KH_2PO_4, 10 mM glucose and 0.25% bovine serum albumin, pH 7.4. ECM with ethylene glycol-bis(β-aminoethyl ether)-*N,N,N′,N′*-tetraacetic acid (EGTA) was prepared by substituting 1 mM $CaCl_2$ by 2.2 mM EGTA. When the dilution medium was ECM with EGTA, free Ca^{2+} in the final mixture was 2.5 nM. For our purposes, this was considered a nominally Ca^{2+}-free medium.

2.3. Ca^{2+} confocal fluorescence

Cells at $\sim 2\times10^4$/plate were seeded onto 35-mm glass bottom plates and maintained at 37 °C for 4 days in the CO_2 incubator. Adherent cells were loaded at 37 °C for either 30 or 60 min in the dark with 2 μM Fluo-4 ester form, washed and left at 25 °C for 30 min to allow complete de-esterification of the probe. Plated cells images were obtained with a Leica Microsystems equipment consisting of a TCS SP2 confocal scanner mounted on a DM IRE II inverted fluorescence microscope. Samples were observed at room temperature through an HCX PL APO 63× oil immersion objective with numerical aperture 1.32. Fluo-4 was excited with the 488 nm argon laser line and the emitted fluorescence was collected through the wavelength interval 504–530 nm. The pinhole aperture was set at 140 μm giving a 1.1 μm thickness of the confocal section. Selected images show planes around the middle of the nuclei.

2.4. Fluorometric measurements with Ca^{2+} probes

The loading medium was ECM with Ca^{2+} supplemented with either 2 μM Fura-2 or dihydroRhod-2, in the ester form, and 0.02% Pluronic® F-127. Sulfinpyrazone at 0.2 mM was included in both the Fura-2 loading medium and the dilution medium for measurements in order to prevent extrusion of the Ca^{2+} probe-free acid. The pH was readjusted every time sulfinpyrazone was added. When Rhod-2 was used a stock aliquot of esterified Rhod-2 was reduced to the nonfluorescent dihydroRhod-2 derivative before loading [24]. The cationic indicator was driven inside the mitochondria by the negative mitochondrial inner membrane potential ($\Delta\Psi_m$) and oxidized to the Ca^{2+}-sensitive Rhod-2. Cells grown on 150-mm tissue culture plates were incubated at 37 °C and in the dark for 30 min with loading medium. After trypsinization, detached cells were washed and resuspended at $\sim 2–4\times10^6$ cells/ml in ECM with Ca^{2+}. The cell suspension was maintained at 25 °C and in the dark for 30 min to allow the Ca^{2+} probe de-esterification. Dye-loaded cells were diluted at the beginning of the experiment to give $\sim 2\times10^5$ cells/ml in the Fura-2 measurements or $\sim 3\times10^5$ cells/ml in the Rhod-2 experiments. When cytoplasmic Ca^{2+} measurements were performed in ECM with Ca^{2+} but without Ni^{2+}, Fura-2-loaded cells were first sedimented at $480\times g$ for 10 min and then resuspended in new ECM with Ca^{2+} just before measurements. This procedure removed fluorescence arising from the external medium due to the passive leak of Fura-2. When samples were diluted in ECM with EGTA or ECM with Ca^{2+} plus 10 mM $NiCl_2$ there was no extracellular fluorescence contribution [23]. The fluorescence signal was recorded at 25 °C in an Aminco-Bowman Series 2 spectrofluorometer, keeping the samples under continuous stirring. Fura-2 fluorescence was obtained by alternate excitation at 340 and 380 nm and the emission was detected at 510 nm. Cytoplasmic free Ca^{2+} was quantified according to the equation derived by Grynkiewicz et al. [25]. Under our assay conditions the apparent dissociation constant for Ca^{2+} binding to Fura-2 was 240 nM [23]. Calibration and background corrections were also made as previously described [23]. Rhod-2 measurements were performed using 550 and 580 nm as excitation and emission wavelengths, respectively. Mitochondrial Ca^{2+} was expressed in arbitrary units as $\Delta F/F\times100$ because calibration of absolute values is not possible with single excitation/emission dyes [26,27].

2.5. Fluorometric measurements with TMRM

Cells detached from 150-mm plates were resuspended in ECM with Ca^{2+} at ~3×10^6 cells/ml. Loading was carried out at 37 °C for 15 min with ECM containing Ca^{2+} and supplemented with 0.2 μM TMRM and 0.02% Pluronic® F-127. Fluorescence intensity at 25 °C was measured after a 10-fold dilution in ECM with Ca^{2+}. The Aminco-Bowman spectrofluorometer was set at 546 and 573 nm as excitation wavelengths while the emission fluorescence was measured at 590 nm. Fluorescence intensity was expressed as the excitation ratio F_{573}/F_{546} of light emitted at 590 nm.

2.6. Cell viability

The assay was based on the ability of living cells to reduce MTT [28]. Cells at ~15×10^3/well were grown at 37 °C for 4 days in 24-well plates. Subconfluent cultures were washed twice with phosphate-buffered saline (PBS) at 37 °C and cells in DMEM were treated with 3 or 10 μM TG. The culture was maintained at 37 °C for defined time intervals and cells were rinsed and incubated for 30 min with 1 mg/ml MTT. The medium was replaced by 250 μl dimethyl sulfoxide and cells were shaken at room temperature and in the dark for 5 min to dissolve the formazan precipitate. Afterwards, each well was supplemented with 25 μl of 2 M Tris, pH 10.5. Aliquots from wells were taken to measure absorbance at 570 nm using a multi-well plate reader (Multiscan MCC/340) from Labsystem and the background absorbance measured at 690 nm was subtracted.

2.7. DNA imaging

Cells at ~15×10^3/coverslip were seeded onto 13-mm round plastic coverslips placed in 24-well plates and maintained at 37 °C for 4 days in the CO_2 incubator. Thereafter, cells were washed twice with PBS at 37 °C and incubated in DMEM containing 3 μM TG. The culture without serum was prolonged at 37 °C for different time periods in the CO_2 incubator. Adherent cells were fixed at room temperature for 5 min with a 1:3 acetic acid/methanol mixture and then incubated for 10 min with PBS containing 5 μg/ml AO and 4% formalin. Coverslips were removed from the wells and inverted onto glass slides containing mounting medium from Sigma. Images were examined with a Leica Microsystems DMRB fluorescence microscope equipped with standard filters. SPOT RT™ digital camera and software were from Diagnostic Instruments, Inc.

2.8. Flow-cytometry with PI staining

Cells grown on 100-mm plates were washed twice with PBS at 37 °C and then incubated in DMEM containing either 3 or 10 μM TG. The culture was maintained at 37 °C and in the CO_2 incubator for different time intervals. For each measurement, one plate containing ~8×10^5 cells was used. The TG treatment led to a variable proportion of cells detachment, therefore the medium with floating cells at the end of each incubation time was reserved and combined with the corresponding trypsinized adherent cells. Pooled cells were pelleted by centrifugation and gently washed with PBS. After fixing at −20 °C for 15 min in cold ethanol, cells were centrifuged, resuspended in PBS and maintained at room temperature for 15 min. Permeabilization and staining was achieved after incubation at room temperature and in the dark for 30 min with PBS containing 5 μg/ml PI, 0.1% Triton X-100 and 50 μg/ml RNase A. Measurements were performed with a FACSort™ flow cytometer from Becton Dickinson. Samples were excited at 488 nm with an argon laser source and fluorescence was detected through a 563–607 nm band pass filter (FL-2 channel). Previously, subcellular debris and cell clumps were electronically gated out using a plot of forward vs. side light scatter. Twenty thousand events (cells) were collected for each measurement and data were analyzed with the Becton Dickinson CellQuest™ software. The sub-G_1 population was taken as the fraction of apoptotic cells.

2.9. Immunoblotting of PARP

Plated cells in DMEM were incubated at 37 °C for the indicated time with 3 or 10 μM TG. Four 150-mm plates containing ~1.5×10^6 cells/plate were used for the preparation of each sample. Treated cells were harvested, washed in ice-cold PBS and resuspended at ~40×10^6 cells/ml in lysis buffer [150 mM Tris–HCl, 1 mM EGTA, 1% Triton X-100, 1% sodium deoxycholate and 0.1% SDS, pH 8.0] along with 100-fold diluted protease inhibitors. The cellular lysate was cleared by brief sonication followed by centrifugation at 10,000×*g* for 10 min and 4 °C. The supernatant fraction was evaluated for protein content by the bicinchoninic acid method [29] before freezing at −80 °C until use. Aliquots of the supernatant fraction were boiled in sample buffer [62.5 mM Tris–HCl, 2% SDS, 5% β-mercaptoethanol, 7.5% glycerol and 0.0003% bromophenol blue, pH 6.8] for 2 min. Thirty μg of protein from each sample were electrophoresed on 7–17% SDS-polyacrylamide gels [30] and transferred to nitrocellulose membrane by a Bio-Rad semi-dry blotting apparatus. Colored markers of the chemichrome western control mix were used to check the protein transfer efficiency. The membrane was treated with signal enhancer reagents and blocked at room temperature for 1 h with PBS containing 5% skim dried milk and 0.05% Tween-20. Incubation with the corresponding primary and secondary antibodies pair preceded blot developing using the chemiluminescent detection system. Anti-PARP antibody was diluted at 1:200 and anti-rabbit IgG conjugated to peroxidase at 1:25,000. The γ-tubulin content in the same membrane was assessed after treatment at 50 °C for 30 min with stripping buffer [62.5 mM Tris–HCl, 2% SDS and 100 mM β-mercaptoethanol, pH 6.8] and re-probing with the corresponding antibodies. Anti-γ-tubulin and anti-mouse IgG conjugated to peroxidase were used at a 1:20,000 dilution. The incubation with

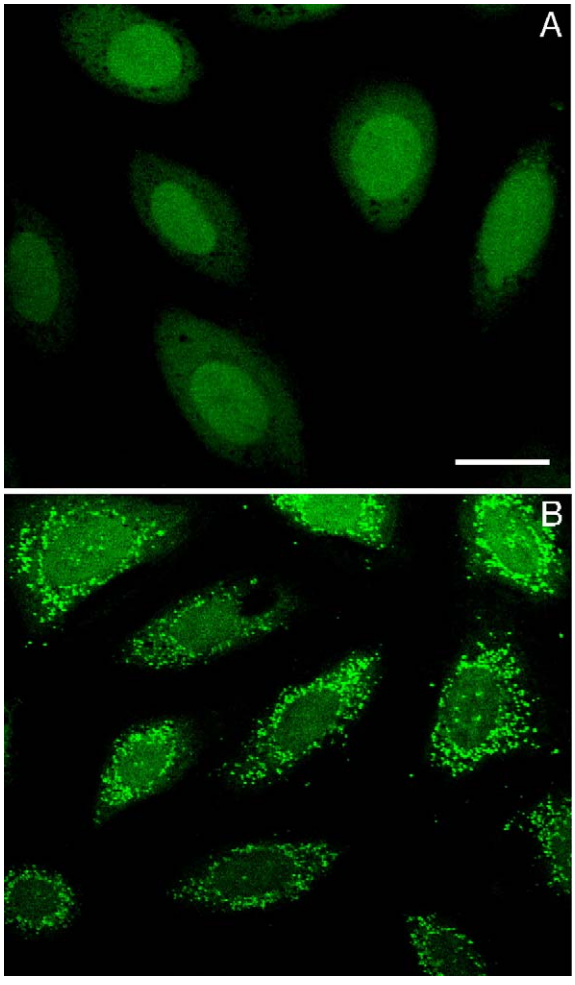

Fig. 1. Time-dependent evolution of the Ca^{2+} fluorescence in H9c2 cells. Plated cells incubated in ECM with Ca^{2+} were loaded at 37 °C for 30 min (A) or 60 min (B) with 2 μM Fluo-4/acetoxymethyl ester. The loading time was followed by a 30 min de-esterification period at 25 °C. Confocal images show representative fields of live cells subjected to different loading times but the same de-esterification period. Bar length in panel A is 50 μm.

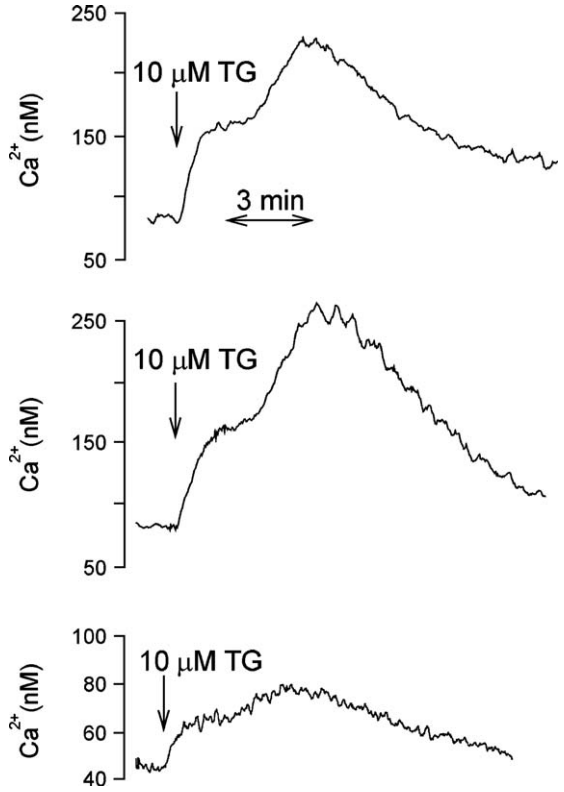

Fig. 2. Time-course of cytoplasmic Ca^{2+} when cells were treated with 10 μM TG. Plated cells were initially loaded with 2 μM Fura-2 and then resuspended in ECM with Ca^{2+}. The fluorescence signal at 25 °C was recorded once the concentrated cells were diluted to give ~2×10^5 cells/ml in the spectrofluorometer cuvette. TG was added when indicated. The dilution medium was ECM with Ca^{2+} (*upper trace*), ECM with Ca^{2+} plus 10 mM $NiCl_2$ (*middle trace*) or ECM with EGTA (*lower trace*). All dilution media were supplemented with 0.2 mM sulfinpyrazone. In the upper trace experiment cells were washed in ECM with Ca^{2+} before measurements.

primary antibody was carried out overnight at 4 °C in a rocker whereas the secondary antibody was incubated at room temperature for 1 h.

2.10. Data presentation

Fluorescence recordings are representative of five or more experiments. Smoothing of the traces was performed using the Savitsky–Golay algorithm. Experimental data points are expressed as mean values plus the standard deviations. Statistical comparison between experimental groups was performed by the Student t-test using SigmaPlot 8.0 software. Values of $P<0.05$ were considered significant. Flow cytometry recordings and blots are representative of repeated experiments performed with more than one sample prepared at each time point.

3. Results

Measurements of cytoplasmic Ca^{2+} are affected by intracellular distribution of the fluorescent probe and this is dependent on cell type and incubation conditions. Thus, the extent of compartmentalization at 37 °C was studied in H9c2 cells using the membrane-permeable derivative of Fluo-4. The intracellular fluorescence distribution was clearly time-dependent. After 30 min of loading the cytoplasm appeared less fluorescent than the nucleus (Fig. 1A) although in some cells the opposite was true. When the loading time was extended to 60 min bright tiny spots were highly abundant within the cytoplasmic region (Fig. 1B). It should be noted that some nuclei also exhibited high fluorescence spots as a consequence of the extended loading period.

The next measurements of cytoplasmic Ca^{2+} were performed taking into account the loading response of the fluorescent probe. Thus, cells in ECM with Ca^{2+} were loaded at 37 °C for 30 min with the cell-permeable Fura-2 ester. Under these conditions, ~80% of the fluorescence was lost by controlled treatment with digitonin [23]. The experimental protocol for quantitative Ca^{2+} measurements was dilution of a concentrated cell suspension in the spectrofluorometer cuvette and addition of the Ca^{2+}-mobilizing agent. Free Ca^{2+} in the cytoplasm at the beginning of the experiments was around 80 nM when ECM with Ca^{2+} was the dilution medium and the addition of a high TG concentration such as 10 μM was followed by the appearance of a two-component cytoplasmic Ca^{2+} peak (Fig. 2). The evolution of the Ca^{2+} transient was dependent on the dilution medium

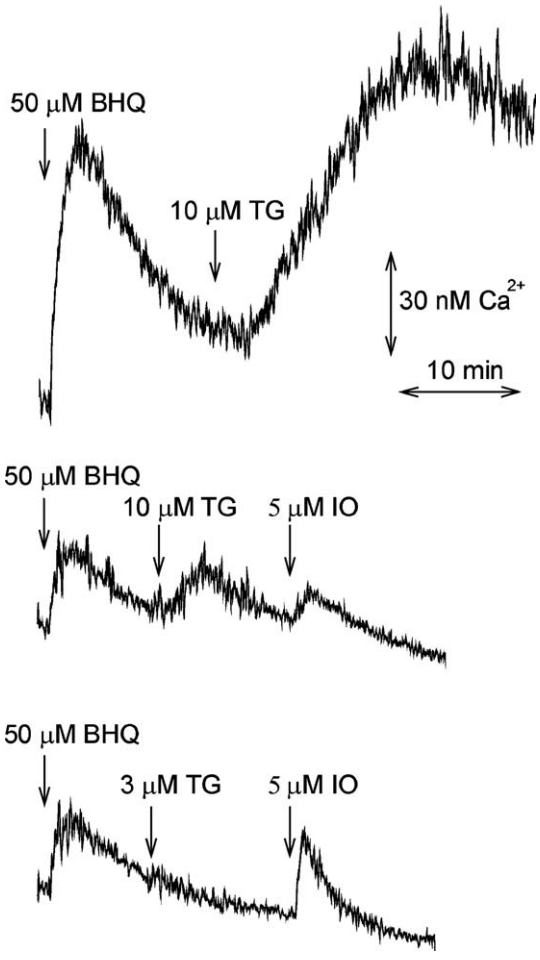

Fig. 3. Cytoplasmic Ca^{2+} response when cells were incubated with Ca^{2+}-mobilizing agents. Cells were preloaded with Fura-2 and then resuspended in ECM with Ca^{2+}. The experiments were initiated by a 10-fold dilution to give ~2×10^5 cells/ml. The dilution medium was ECM with Ca^{2+} plus 10 mM Ni^{2+} (*upper trace*) or ECM with EGTA (*middle and lower trace*). Additions of BHQ, TG or IO were made when indicated. Sulfinpyrazone was maintained at 0.2 mM after dilution.

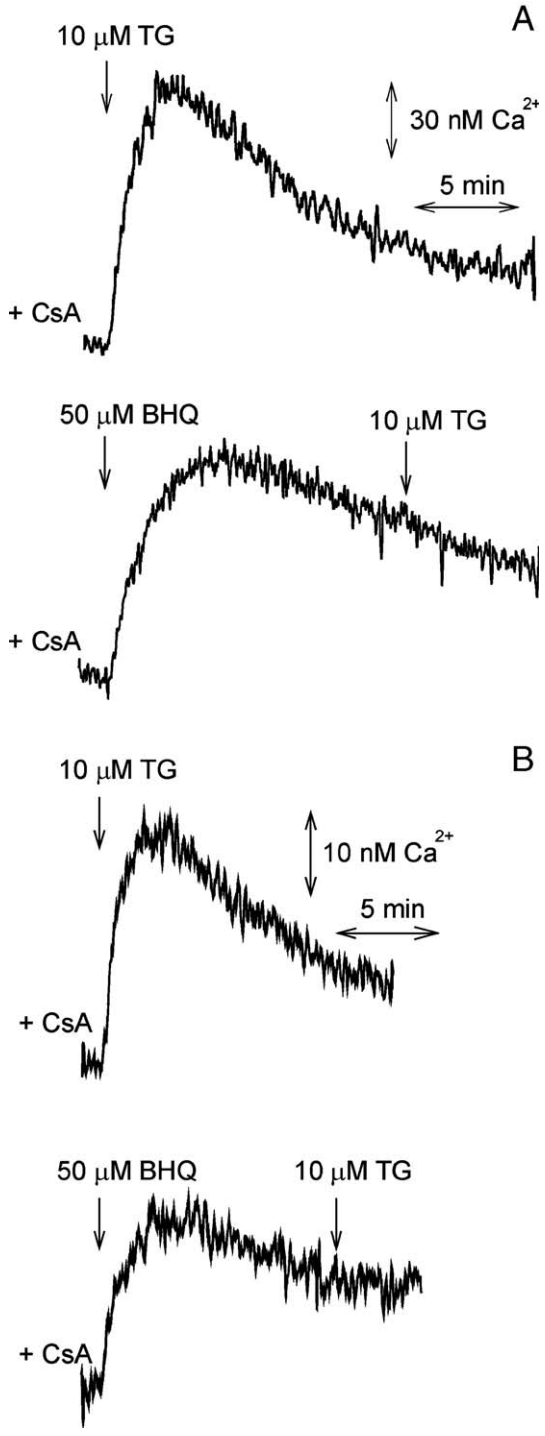

Fig. 4. Effect of Ca^{2+}-mobilizing agents on cytoplasmic Ca^{2+} measured in the presence of CsA. Cells loaded with Fura-2 were diluted 10-fold at the beginning of the experiment. (A) The dilution medium was ECM with Ca^{2+} plus 10 mM Ni^{2+} and 0.2 mM sulfinpyrazone. (B) The dilution medium was ECM with EGTA supplemented with 0.2 mM sulfinpyrazone. After dilution, 5 μM CsA was added and a 10 min time span was allowed before the addition of any Ca^{2+}-mobilizing agent.

composition (cf. *upper* with *middle* trace). The cytoplasmic Ca^{2+} rise tended to return to the initial resting level when Ni^{2+} was present to avoid the capacitative Ca^{2+} entry [23]. Likewise, the initial free Ca^{2+} in the cytoplasm was ~45 nM and the magnitude of the transient Ca^{2+} rise was smaller when cells were diluted in ECM with EGTA (cf. *upper* and *middle traces* with *lower trace* in Fig. 2).

The unexpected profile induced by 10 μM TG prompted us to analyze in more detail the cytoplasmic Ca^{2+} response. This was approached by using an alternative agent, BHQ, to discharge the SER Ca^{2+} store [31]. The addition of 50 μM BHQ to cells diluted in ECM with Ca^{2+} plus 10 mM Ni^{2+} was followed by the appearance of a single cytoplasmic Ca^{2+} peak (Fig. 3, *upper trace*) and the subsequent addition of 10 μM TG provided now a one-component Ca^{2+} peak. In fact, the two independent Ca^{2+} peaks observed after the sequential addition of 50 μM BHQ and 10 μM TG in the presence of extracellular Ca^{2+} were also reproduced when the experiments were repeated in a Ca^{2+}-free medium (Fig. 3, *middle trace*). The mobilization of intracellular Ca^{2+} was smaller in the latter case and some Ca^{2+} from intracellular pools was still released after the subsequent addition of 5 μM IO. The cytoplasmic Ca^{2+} response was also studied adding first 50 μM BHQ and then 3 μM TG and using ECM with EGTA as dilution medium. In this case, the addition of 3 μM TG did not elicit any Ca^{2+} response when added once the Ca^{2+} peak triggered by 50 μM BHQ was observed (Fig. 3, *lower trace*). Here again, the later addition of 5 μM IO was able to release Ca^{2+}.

The identity of the second component in the cytoplasmic Ca^{2+} response induced by 10 μM TG was then explored using the PTP inhibitor CsA [32]. In these experiments, cells diluted

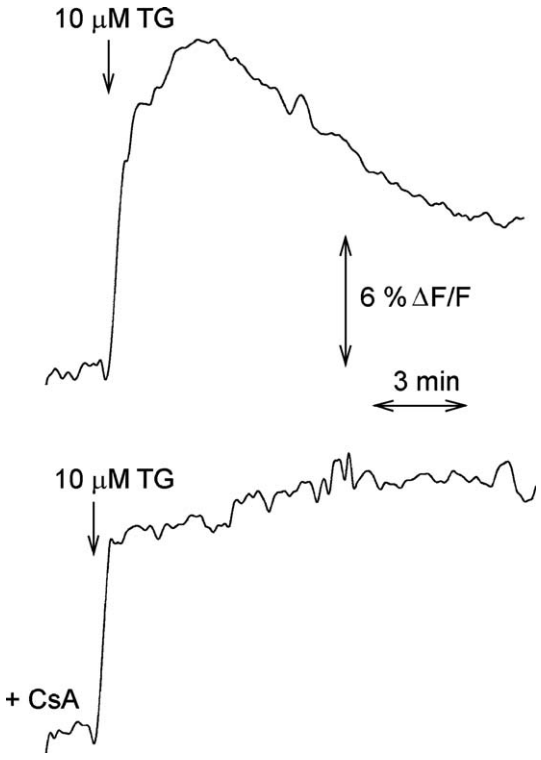

Fig. 5. Time-dependent effect of mitochondrial Ca^{2+} when cells were treated with 10 μM TG. Plated cells were loaded with dihydroRhod-2 and concentrated in suspension using ECM with Ca^{2+}. Cells aliquots were diluted 10-fold in ECM with EGTA to give ~3×10^5 cells/ml and 2.5 nM free Ca^{2+}. TG at 10 μM was added when indicated. In the lower trace experiment the addition of 10 μM TG was preceded by 10 min incubation with 5 μM CsA.

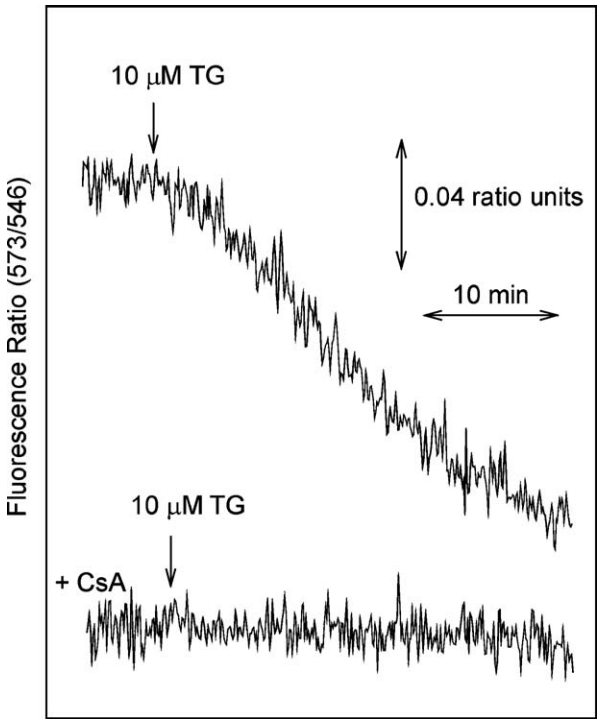

Fig. 6. Effect of 10 μM TG on TMRM fluorescence of H9c2 cells. Plated cells were loaded with 0.2 μM TMRM and then resuspended in ECM with Ca^{2+}. Cells were diluted in ECM with Ca^{2+} to yield ~3×10^5 cells/ml and excited at F_{573}/F_{546}. The fluorescence emission at 590 nm was recorded as a function of time once the loaded cells were diluted 10-fold in ECM with Ca^{2+}. TG at 10 μM was added when indicated. In the lower trace experiment the addition of 10 μM TG was preceded by 10 min incubation with 5 μM CsA.

in ECM with Ca^{2+} plus 10 mM Ni^{2+} were supplemented with 5 μM CsA and 10 min later the cytoplasmic Ca^{2+} response was evoked by adding 10 μM TG. Our data show the appearance of a single peak corresponding to the first component of the Ca^{2+} signal (Fig. 4A, *upper trace*). Clearly, preincubation with CsA abolished the second component. Additional evidence was given by adding first 50 μM BHQ and then 10 μM TG to cells preincubated for 10 min with 5 μM CsA. The BHQ addition evoked the first component of the cytoplasmic Ca^{2+} signal and 10 μM TG did not elicit any further response (Fig. 4A, *lower trace*). Parallel experiments were carried out in a Ca^{2+}-free medium and the 10 min preincubation with 5 μM CsA was also performed as before. The cytoplasmic Ca^{2+} response was qualitatively similar to that observed when ECM with Ca^{2+} plus 10 mM Ni^{2+} was used. Namely, 10 μM TG elicited the first component of the Ca^{2+} signal when cells were preincubated with CsA and no effect was observed when cells preincubated with CsA were previously treated with 50 μM BHQ (Fig. 4B).

The mitochondrial Ca^{2+} response after addition of TG was monitored using the fluorescent probe Rhod-2. These experiments were performed using ECM with EGTA as dilution medium to rule out any Ca^{2+} contribution from the extracellular space. Thus, addition of 10 μM TG to Rhod-2-loaded cells was sensed as a mitochondrial Ca^{2+} transient. An initial increase of the mitochondrial Ca^{2+} pool was followed by a slower decrease (Fig. 5, *upper trace*). When the experiment was repeated but cells were previously treated for 10 min with 5 μM CsA the 10 μM TG addition produced a mitochondrial Ca^{2+} rise that was maintained in the following min (Fig. 5, *lower trace*).

Additional information was afforded by measuring the fluorescence of cells loaded with TMRM as a semiquantitative probe of $\Delta\Psi_m$ [33]. The kinetics of TMRM-loaded cells showed that the addition of 10 μM TG to cells diluted in ECM with Ca^{2+} was followed by a progressive decrease of the TMRM fluorescence, an event occurring in the min time scale (Fig. 6, *upper trace*). Interestingly, the TMRM fluorescence was insensitive to 10 μM TG when cells were previously incubated for 10 min with 5 μM CsA (Fig. 6, *lower trace*).

The impact of the TG treatment on cell viability was assayed by measuring the mitochondrial function with the MTT reagent. Thus, when cells were incubated with 3 μM TG (Fig. 7A, closed bars) or 10 μM TG (Fig. 7B, closed bars) there was a clear time-

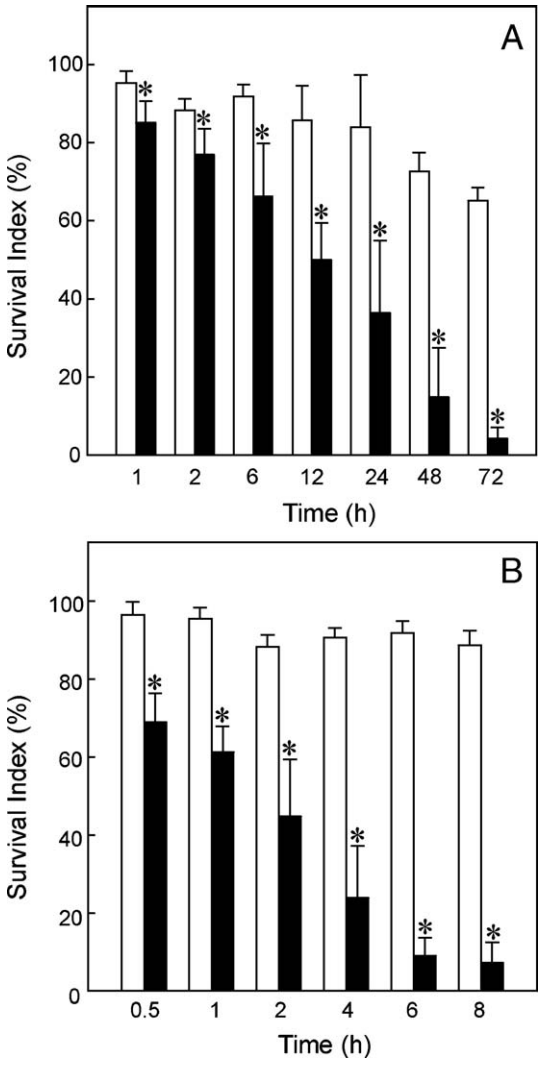

Fig. 7. Effect of the TG treatment on cell viability using the MTT assay. Cells in 24-well plates were cultured at 37 °C in DMEM containing 3 (A) or 10 μM TG (B). The incubation was maintained for different time intervals and then samples were processed for formazan quantification. Cells subjected to TG treatment are shown as closed bars. Untreated cells subjected to the same manipulation but in the absence of TG correspond to open bars. The index of cell survival is expressed as a percentage of a time zero control. Statistically significant effect of TG, when compared to untreated cells at each time point (*).

dependent decrease on cell viability. Unfold of the noxious effect was dependent on the insult dosage received by the cells. Full loss of viability required ~72 h when 3 μM TG was used whereas a similar effect was developed in ~8 h when the TG concentration was 10 μM. Serum removal from the culture medium was associated with a certain loss of cell viability, an effect that was more evident when the incubation time was prolonged (cf. open bars in Fig. 7A and B).

The MTT assay did not inform on cell death mechanism therefore additional assays were performed to discriminate between apoptotic and non-apoptotic death. A hallmark of apoptosis is condensation and fragmentation of the nuclear chromatin and this was analyzed by fluorescence microscopy [34]. In these experiments, cells were incubated at 37 °C with 3 or 10 μM TG and the incubation was prolonged for different time intervals before fixation and staining with AO. The main panel of Fig. 8 shows a representative field of cells treated for 48 h with 3 μM TG. As can be seen, the apoptotic nuclear morphology is apparent in a significant number of cells. The small panels on the right show individual nuclei in different stages of the apoptotic process. The same nuclear morphology but in a shorter time span was developed under the presence of 10 μM TG (data not shown).

Chromatin staining and flow cytometry can be used to quantify the cellular DNA content [34]. To this end, cells were incubated at 37 °C with 3 or 10 μM TG for the indicated time and the fluorescence of cells stained with PI was analyzed. Cells were properly gated to select the main population. Representative experiments on DNA content are shown in Fig. 9A and B. Panel B corresponds to cells treated for 48 h with 3 μM TG whereas panel A is the corresponding control, i.e., cells incubated for 48 h but in the absence of TG. Data displayed as histogram representation indicate that the larger fraction in the control experiment (panel A) corresponds to diploid cells or G_1 peak with some contribution of hyperdiploid cells located at the S phase and the G_2/M peak. A minor proportion of hypodiploid cells related with spontaneous apoptosis also appeared as the sub-G_1 population. The sub-G_1 population amounted to 3% when expressed as percentage with respect to the total cell number. However, the sub-G_1 population increased to 26% when cells were incubated for 48 h in the presence of 3 μM TG (panel B).

The extension of the apoptotic effect is also displayed when cells were treated with TG for different time intervals. The apoptotic cell population, measured as the sub-G_1 population, increased as a function of time when cells were exposed to 3 μM TG (Fig. 9C, closed bars). It is also shown that apoptosis was developed in a shorter time span when 10 μM TG was used (Fig. 9D, closed bars). The apoptotic phenomenon developed in the absence of TG was also evaluated in control experiments. Spontaneous apoptosis at each incubation time represented a small proportion (see open bars in Fig. 9C and D).

A prominent feature of the apoptotic execution phase is the selective cleavage of the nuclear enzyme PARP by caspase 3 [35]. The cleavage of the full length PARP (116 kDa) is accompanied by the accumulation of a 85 kDa fragment that can be detected by immunoblotting. Treatment of H9c2 cells with TG had a direct effect on the 116 kDa protein that can be detected with anti-PARP antibody. The proteolytic cleavage of PARP was noticed after 12 h when cells were exposed to 3 μM TG (Fig. 10). However, the accumulation of the p85 fragment was clearly observed at ~3 h when the TG concentration was 10 μM.

The direct link between mitochondrial dysfunction and the faster apoptotic death was established by studying the protective role of CsA. As can be seen (Fig. 11A), the time-dependent decrease of the survival index, when cells were treated with 10 μM TG, was clearly prevented when 5 μM CsA was added 10 min before TG. It is worth to mention that protection afforded by CsA was gradually lost as a function of time. Thus, protection at 4 h was lower than at 2 h. Likewise, addition of CsA alone induced a slight deleterious effect. Data shown at each time point were expressed with respect to the corresponding value of untreated cells maintained in DMEM,

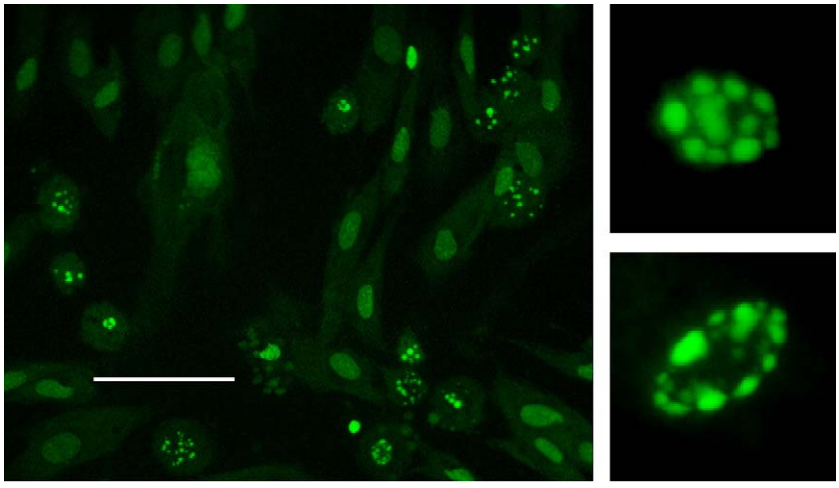

Fig. 8. Effect of the TG treatment on the nucleus morphology using the chromatin probe AO. Cells attached to round coverslip were cultured at 37 °C for 48 h in DMEM containing 3 μM TG. Thereafter, adherent cells were fixed with acetic acid/methanol and stained for 10 min with 5 μg/ml AO. The green fluorescence was captured by a Leica microscope. Small panels on the right show details of the nuclear morphology. The bar in the main field is 50 μm. (For interpretation of the references to colour in this figure legend, the reader is referred to the web version of this article.)

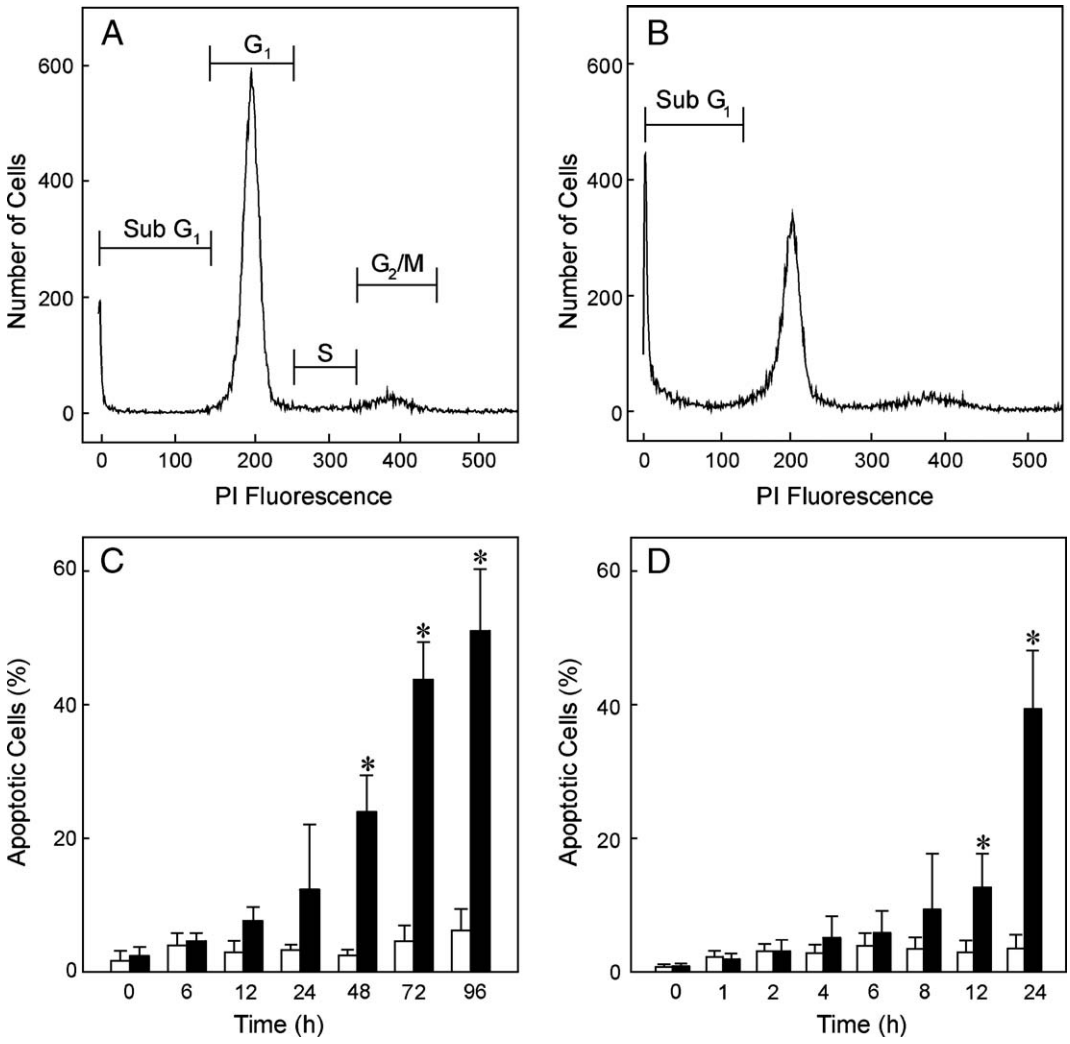

Fig. 9. Effect of the TG treatment on DNA content after staining with PI. Plated cells were cultured at 37 °C for different time intervals in DMEM containing 3 or 10 μM TG. Thereafter, all cells were recovered, fixed with cold ethanol and treated with PBS containing Triton X-100, PI and RNase A. Cells labelled with PI were analyzed by flow-cytometry after gating the cell population. Upper panels correspond to typical measurements of DNA content when cells were cultured in the presence of 3 μM TG for 48 h (B) or subjected to the same procedure but in the absence of TG (A). Lower panels show data on apoptotic cells as a function of the treatment duration with 3 μM TG (C) or 10 μM (D). Closed bars show apoptosis values in the presence of TG and open bars are control values when cells were treated in the absence of TG. Statistically significant effect of TG, when compared to control cells at each time point (*).

i.e., in the absence of serum. CsA also retarded the proteolytic cleavage of PARP induced by 10 μM TG. Thus, the appearance of the p85 fragment, that was visible after 3 h as a consequence of the TG treatment (see, lower blot in Fig. 10), was delayed to 12 h when cells were preincubated for 10 min with 5 μM CsA before the TG addition (Fig. 11B). It means that the time course of PARP cleavage induced by 10 μM TG in the presence of CsA was coincident with that observed in the presence of 3 μM TG.

4. Discussion

The time-course of cell loading at 37 °C with Fluo-4/acetoxymethyl ester was monitored by confocal microscopy. A representative field taken after 30 min of loading confirmed the presence of a low and diffuse fluorescence in the cytoplasm (Fig. 1A) that can be attributed to the low Ca^{2+} level in the resting state. It was also noted that the nuclear region appeared brighter. Higher fluorescence intensity in the nucleus than in the cytoplasm has been attributed to different fluorescence properties of the probe [36]. When the loading time was maintained for 60 min, a spotty fluorescence pattern in the cytoplasm consistent with compartmentalization and high Ca^{2+} concentration in specific stores was apparent (Fig. 1B). The compartmentalized fluorescence can be mainly ascribed to Ca^{2+} stored in the SER but trapping of the dye in the mitochondria cannot be excluded. Fluo-4 is the probe of choice to observe intracellular distribution but not for quantitative measurements. Therefore, quantitative measurements were performed with the ratiometric Ca^{2+} probe Fura-2.

Inhibition of the SER Ca^{2+}-ATPase by TG is a well-known process associated with cytoplasmic Ca^{2+} overload [20,21]. Full inhibition of the SER Ca^{2+}-ATPase was observed at subnanomolar TG concentrations [37] although the same low TG concentration may also stimulate the activity of the P-glycoprotein ATPase [38]. Effect of TG on other targets has also been reported at higher concentrations [39,40].

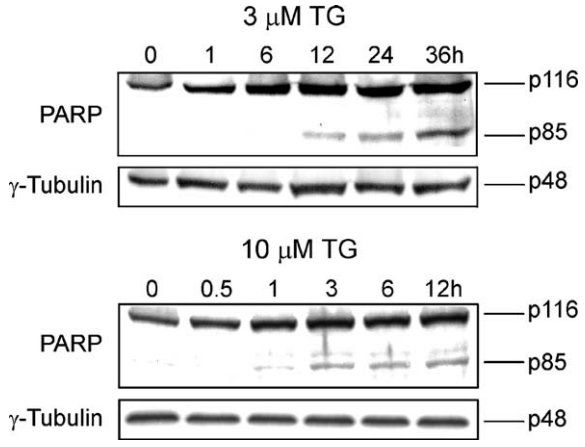

Fig. 10. Effect of the TG treatment on PARP processing. Plated cells in DMEM were exposed at 37 °C for different time intervals to 3 or 10 μM TG. Aliquots of each solubilized cell lysate were subjected to electrophoretic separation and electro-blotting for the immunodetection of PARP. Full length PARP (p116) and the cleavage product (p85) are indicated. The same membranes were stripped and re-probed with anti-γ-tubulin to check the loading of the lanes.

Previous studies with H9c2 cells have indicated that maximal Ca^{2+} release was achieved by at least 100 nM TG when $\sim 2 \times 10^5$ cells/ml were present. Indeed, the addition of up to 3 μM TG gave rise to a single cytoplasmic Ca^{2+} peak [23]. The present data reveal that the addition of 10 μM TG elicits a two-component Ca^{2+} peak (Fig. 2). The first component of the signal was coincident in time and extension with that induced by 3 μM TG and the second component appeared later and was partially overlapped with the first one. The two-component rise was observed whether or not Ca^{2+} was present in the dilution medium confirming the intracellular origin of the signal.

The maximal cytoplasmic Ca^{2+} response of H9c2 cells to BHQ was previously observed at ≥50 μM [23]. Thus, the initial discharge of the SER Ca^{2+} store by 50 μM BHQ led to the subsequent appearance of a single cytoplasmic Ca^{2+} peak when 10 μM TG was added whereas a lack of response was observed when 3 μM TG was used (Fig. 3). The single Ca^{2+} peak induced by 10 μM TG was observed when the experiments were performed in the presence or absence of Ca^{2+}. Likewise, the lack of effect when 3 μM TG was added following exposure to 50 μM BHQ was not related with total depletion of the intracellular Ca^{2+} pools. This was proved by the appearance of a Ca^{2+} peak after addition of the selective Ca^{2+} ionophore IO.

When cells were preincubated with CsA, added to block the opening of the PTP, the addition of 10 μM TG elicited a single cytoplasmic Ca^{2+} peak (Fig. 4). This was the same behaviour observed when 3 μM TG was added to untreated H9c2 cells [23]. Consequently, when 50 μM BHQ was initially added to discharge the SER Ca^{2+} store, the later addition of 10 μM TG failed to induce any response. The selective effect of 10 μM TG on the SER Ca^{2+} store when the PTP was blocked and the lack of effect when 50 μM BHQ was previously added was also observed in the absence of external Ca^{2+}. These data suggest that the second component of the cytoplasmic Ca^{2+} response is of mitochondrial origin.

The mitochondrial Ca^{2+} response after the 10 μM TG addition was associated with Ca^{2+} entry and gave rise to a transient accumulation that tended to decrease more slowly (Fig. 5). Preincubation with CsA prevented the release of mitochondrial Ca^{2+}. These data indicate that 10 μM TG was able to open the PTP thus eliciting a delayed release of mitochondrial Ca^{2+}. This was consistent with the sensitivity of the second component of the cytoplasmic Ca^{2+} peak to CsA.

The second component of the Ca^{2+} peak can be attributed to a direct action of TG on the mitochondria. An indirect effect through the SER provoked by the close association between SER and mitochondria can be excluded since the selective discharge of the SER Ca^{2+} store by BHQ did not elicit the second component under any circumstance.

The effect of 10 μM TG as inducer of PTP opening was also manifested by the TMRM fluorescence measurements. The presence of 10 μM TG was associated with a large and sustained depolarization of the mitochondrial inner membrane (Fig. 6). The TG-induced fall of $\Delta \Psi_m$ was abolished when cells were

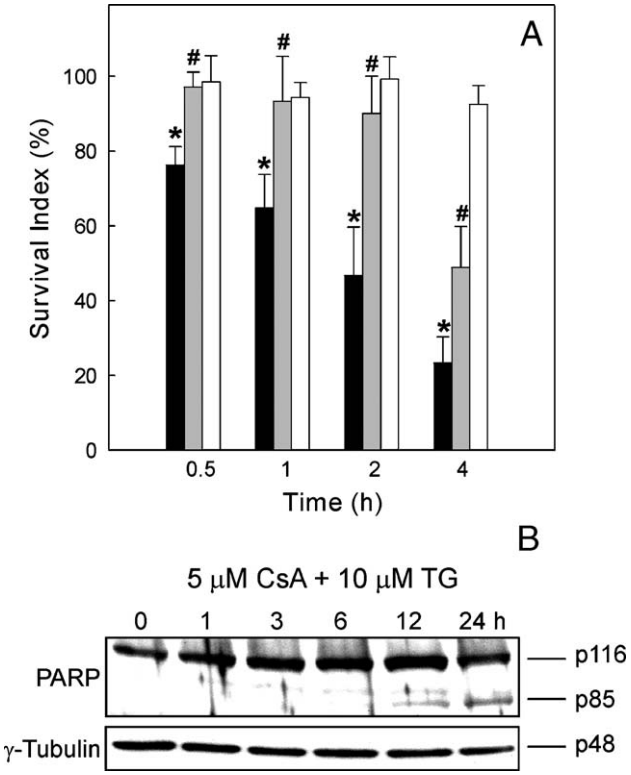

Fig. 11. Effect of CsA on cell damage and PARP cleavage induced by 10 μM TG. (A) Cells in 24-well plates were incubated at 37 °C for different time periods in DMEM and then processed for the MTT assay. The incubation medium was supplemented with 10 μM TG (closed bars), 10 μM TG plus 10 min preincubation with 5 μM CsA (gray bars) or 5 μM CsA added in preincubation for 10 min (open bars). The survival index at each time point was referred to the corresponding value of control cells maintained in DMEM. Statistically significant effect of TG, when compared to cells measured at the same time span but in the absence of TG (*); statistically significant effect of CsA, when compared to cells treated with TG for the same time span but in the absence of CsA (#). (B) Time course of PARP cleavage when cells in DMEM were preincubated for 10 min with 5 μM CsA and then exposed to 10 μM TG. Full length and large fragment of PARP are p116 and p85, respectively. The γ-tubulin content (p48) in the same membrane is shown as a control of loading.

preincubated with CsA. In this regard, the addition of 3 μM TG producing a selective effect on the SER gave a very small and reversible drop of $\Delta\Psi_m$ [23].

It was recognized in *Trypanosoma brucei* and also in isolated rat liver mitochondria that >10 μM TG induces Ca^{2+} release from the mitochondrial store and the observed release was associated with a fall of $\Delta\Psi_m$ [39]. Evidence has also been provided that Ca^{2+} release from isolated heart and liver mitochondria induced by 15–20 μM TG can be inhibited by CsA [40]. These studies concluded that the TG-induced Ca^{2+} release from mitochondria occurred through the PTP.

The distinct concentration-dependent effect of TG on cytoplasmic Ca^{2+} signals was confirmed by measuring cell viability (Fig. 7). Full loss of viability was developed in a shorter time window when the TG concentration was 10 μM as compared with 3 μM. In any case, chromatin fragmentation and margination at the nuclear periphery (Fig. 8), loss of DNA content (Fig. 9) and specific cleavage of the caspase 3 substrate PARP (Fig. 10) was the experimental evidence that the cellular death mechanism induced by different TG concentrations was apoptosis.

The onset of the TG-induced apoptosis in H9c2 cells was delayed when 3 μM TG was used instead of 10 μM. This suggests that different TG concentrations are able to affect different targets. A lower TG concentration illustrated by 3 μM and affecting the SER Ca^{2+} store elicited cell death but a higher TG concentration represented by 10 μM and affecting the mitochondrial PTP was a faster deadly stimulus. In this sense, the second component of the cytoplasmic Ca^{2+} peak which is related with Ca^{2+} release from the mitochondria seems to be the consequence of the PTP opening rather than the cause.

The involvement of PTP opening in the faster apoptotic process was confirmed by studying the effect of CsA when added before the 10 μM TG treatment. CsA retarded cell damage measured by the MTT assay and apoptosis progression detected by PARP cleavage (Fig. 11). The decrease in cell damage protection observed at 4 h can be related with the transient effect of CsA as a PTP blocker [41] and also with the appearance of the slower apoptotic process caused by the first component of the cytoplasmic Ca^{2+} peak. The use of CsA to prove the participation of PTP must be taken with some caution because other targets and cellular effects have been described. Evaluation of the 5 μM CsA effect during the early time frame confirmed a very small cell damage induced by the drug.

PTP opening and the subsequent release of mitochondrial content are relevant to the pathophysiology of myocardiac cells. Several studies have reported the key role of PTP opening in cardiac reperfusion injury after a period of ischemia [42–44]. In fact, heart damage associated with reperfusion can be protected by pretreatment with CsA [42–44]. Studies are in progress to identify cellular events underlying the TG-induced apoptotic cascades.

Acknowledgments

We thank Dr. Garcia-Estan and Dr. Marín Atucha from the School of Medicine Department of Physiology for the use of the Aminco-Bowman spectrofluorometer. This work was supported by grant BMC2002-02474 from the Spanish Ministerio de Educación y Ciencia/Fondo Europeo de Desarrollo Regional and by a grant-in-aid from the Universidad de Murcia.

References

[1] M.J. Berridge, M.D. Bootman, P. Lipp, Calcium—A life and death signal, Nature 395 (1998) 645–648.
[2] H. Cheng, W.J. Lederer, M.B. Cannell, Calcium sparks: elementary events underlying excitation–contraction coupling in heart muscle, Science 262 (1993) 740–744.
[3] Y. Yao, J. Choi, I. Parker, Quantal puffs of intracellular Ca^{2+} evoked by inositol trisphosphate in *Xenopus* oocytes, J. Physiol. 482 (1995) 533–553.
[4] M.J. Berridge, M.D. Bootman, H.L. Roderick, Calcium signalling: dynamics, homeostasis and remodelling, Nat. Rev., Mol. Cell Biol. 4 (2003) 517–529.
[5] S. Boitano, E.R. Dirksen, M.J. Sanderson, Intercellular propagation of calcium waves mediated by inositol trisphosphate, Science 258 (1992) 292–295.
[6] L.D. Robb-Gaspers, A.P. Thomas, Coordination of Ca^{2+} signaling by intercellular propagation of Ca^{2+} waves in the intact liver, J. Biol. Chem. 270 (1995) 8102–8107.
[7] M.D. Bootman, M.J. Berridge, The elemental principles of calcium signalling, Cell 83 (1995) 675–678.
[8] R.E. Dolmetsch, R.S. Lewis, C.C. Goodnow, J.I. Healy, Differential activation of transcription factors induced by Ca^{2+} response amplitude and duration, Nature 384 (1977) 855–858.
[9] B.J. Wilkins, Y.-S. Dai, O.F. Bueno, S.A. Parsons, J. Xu, D.M. Plank, F. Jones, T.R. Kimball, J.D. Molkentin, Calcineurin/NFAT coupling participates in pathological, but not physiological, cardiac hypertrophy, Circ. Res. 94 (2004) 110–118.
[10] J.A. Lee, D.G. Allen, Changes in intracellular free calcium concentration during long exposures to simulated ischemia in isolated mammalian ventricular muscle, Circ. Res. 71 (1992) 58–69.
[11] M.R. Duchen, Mitochondria and calcium: from cell signalling to cell death, J. Physiol. 529 (2000) 57–68.
[12] P. Pacher, G. Csordás, G. Hajnóczky, Mitochondrial Ca^{2+}-signaling and cardiac apoptosis, Biol. Signals Recept. 10 (2001) 200–223.
[13] W. Cheng, J. Kajstura, J.A. Nitahara, B. Li, K. Reiss, Y. Liu, W.A. Clark, S. Krajewski, J.C. Reed, G. Olivetti, P. Anversa, Programmed myocyte cell death affects the viable myocardium after infarction in rats, Exp. Cell Res. 226 (1966) 316–327.
[14] V.G. Sharov, H.N. Sabbah, H. Shimoyama, A.V. Goussev, M. Lesch, S. Goldstein, Evidence of cardiocyte apoptosis in myocardium of dogs with chronic heart failure, Am. J. Pathol. 148 (1996) 141–149.
[15] E. Teiger, T.-V. Dam, L. Richard, C. Wisnewsky, B.-S. Tea, L. Gaboury, J. Tremblay, K. Schwartz, P. Hamet, Apoptosis in pressure overload-induced heart hypertrophy in the rat, J. Clin. Invest. 97 (1996) 2891–2897.
[16] P.M. Kang, A. Haunstetter, H. Aoki, A. Usheva, S. Izumo, Morphological and molecular characterization of adult cardiomyocyte apoptosis during hypoxia and reoxygenation, Circ. Res. 87 (2000) 118–125.
[17] O. Thastrup, B. Foder, O. Scharff, The calcium mobilizing and tumor promoting agent, thapsigargin elevates the platelet cytoplasmic free calcium concentration to a higher steady state level. A possible mechanism of action for the tumor promotion, Biochem. Biophys. Res. Commun. 142 (1987) 654–660.
[18] T.R. Jackson, S.I. Patterson, O. Thastrup, M.R. Hanley, A novel tumour promoter, thapsigargin, transiently increases cytoplasmic free Ca^{2+} without generation of inositol phosphates in NG115-401L neuronal cells, Biochem. J. 253 (1988) 81–86.
[19] M.S. Kirby, Y. Sagara, S. Gaa, G. Inesi, W.J. Lederer, T.B. Rogers, Thapsigargin inhibits contraction and Ca^{2+} transient in cardiac cells by specific inhibition of the sarcoplasmic reticulum Ca^{2+} pump, J. Biol. Chem. 267 (1992) 12545–12551.

[20] S. Jiang, S.C. Chow, P. Nicotera, S. Orrenius, Intracellular Ca^{2+} signals activate apoptosis in thymocytes: studies using the Ca^{2+}-ATPase inhibitor thapsigargin, Exp. Cell Res. 212 (1994) 84–92.
[21] Y. Furuya, P. Lundmo, A.D. Short, D.L. Gill, J.T. Isaacs, The role of calcium, pH, and cell proliferation in the programmed (apoptotic) death of androgen-independent prostatic cancer cells induced by thapsigargin, Cancer Res. 54 (1994) 6167–6175.
[22] X.-M. Qi, H. He, H. Zhong, C.W. Distelhorst, Baculovirus p35 and z-VAD-fmk inhibit thapsigargin-induced apoptosis of breast cancer cells, Oncogene 15 (1997) 1207–1212.
[23] A. Lax, F. Soler, F. Fernández-Belda, Intracellular Ca^{2+} pools and fluxes in cardiac muscle-derived H9c2 cells, J. Bioenerg. Biomembranes 37 (2005) 249–259.
[24] D.N. Bowser, T. Minamikawa, P. Nagley, D.A. Williams, Role of mitochondria in calcium regulation of spontaneously contracting cardiac muscle cells, Biophys. J. 75 (1998) 2004–2014.
[25] G. Grynkiewicz, M. Poenie, R.Y. Tsien, A new generation of Ca^{2+} indicators with greatly improved fluorescence properties, J. Biol. Chem. 260 (1985) 3440–3450.
[26] G. Hajnóczky, L.D. Robb-Gaspers, M.B. Seitz, A.P. Thomas, Decoding of cytosolic calcium oscillations in the mitochondria, Cell 82 (1995) 415–424.
[27] G.R. Monteith, M.P. Blaustein, Heterogeneity of mitochondrial matrix free Ca^{2+}: resolution of Ca^{2+} dynamics in individual mitochondria in situ, Am. J. Physiol. 276 (1999) C1193–C1204.
[28] T. Mosmann, Rapid colorimetric assay for cellular growth and survival: application to proliferation and cytotoxicity assays, J. Immunol. Methods 65 (1983) 55–63.
[29] P.K. Smith, R.I. Krohn, G.T. Hermanson, A.K. Mallia, F.H. Gartner, M.D. Provenzano, E.K. Fujimoto, N.M. Goeke, B.J. Olson, D.C. Klenk, Measurement of protein using bicinchoninic acid, Anal. Biochem. 150 (1985) 76–85.
[30] U.K. Laemmli, Cleavage of structural proteins during the assembly of the head of bacteriophage T4, Nature 227 (1970) 680–685.
[31] G.E.N. Kass, S.K. Duddy, G.A. Moore, S. Orrenius, 2,5-Di-(*tert*-butyl)-1,4-benzohydroquinone rapidly elevates cytosolic Ca^{2+} concentration by mobilizing the inositol 1,4,5-trisphosphate-sensitive Ca^{2+} pool, J. Biol. Chem. 254 (1989) 15192–15198.
[32] M. Crompton, H. Ellinger, A. Costi, Inhibition by cyclosporin A of a Ca^{2+}-dependent pore in heart mitochondria activated by inorganic phosphate and oxidative stress, Biochem. J. 255 (1988) 357–360.
[33] R.C. Scaduto, L.W. Grotyohann, Measurement of mitochondrial membrane potential using fluorescent rhodamine derivatives, Biophys. J. 76 (1999) 469–477.
[34] A.J. McGahon, S.J. Martin, R.P. Bissonnette, A. Mahboubi, Y. Shi, R.J. Mogil, W.K. Nishioka, D.R. Green, The end of the (cell) line: methods for the study of apoptosis in vitro, Methods Cell Biol. 46 (1995) 153–185.
[35] M. Tewari, L.T. Quan, K. O'Rourke, S. Desnoyers, Z. Zeng, D.R. Beidler, G.G. Poirier, G.S. Salvesen, V.M. Dixit, Yama/CPP32β, a mammalian homolog of CED-3, is a CrmA-inhibitable protease that cleaves the death substrate poly(ADP-ribose) polymerase, Cell 81 (1995) 801–809.
[36] C. Perez-Terzic, L. Stehno-Bittel, D.E. Clapham, Nucleoplasmic and cytoplasmic differences in the fluorescence properties of the calcium indicator Fluo-3, Cell Calcium 21 (1997) 275–282.
[37] Y. Sagara, G. Inesi, Inhibition of the sarcoplasmic reticulum Ca^{2+} transport ATPase by thapsigargin at subnanomolar concentrations, J. Biol. Chem. 266 (1991) 13503–13506.
[38] C. Xu, H. Ma, G. Inesi, M.K. Al-Shawi, C. Toyoshima, Specific structural requirements for the inhibitory effect of thapsigargin on the Ca^{2+}-ATPase SERCA, J. Biol. Chem. 279 (2004) 17973–17979.
[39] A.E. Vercesi, S.N.J. Moreno, C.F. Bernardes, A.R. Meinicke, E.C. Fernandes, R. Docampo, Thapsigargin causes Ca^{2+} release and collapse of the membrane potential of *Trypanosoma brucei* mitochondria in situ and of isolated rat liver mitochondria, J. Biol. Chem. 268 (1993) 8564–8568.
[40] P. Korge, J.N. Weiss, Thapsigargin directly induces the mitochondrial permeability transition, Eur. J. Biochem. 265 (1999) 273–280.
[41] N. Zamzami, G. Kroemer, The mitochondrion in apoptosis: how Pandora's box opens, Nat. Rev., Mol. Cell Biol. 2 (2001) 67–71.
[42] E.J. Griffiths, A.P. Halestrap, Protection by cyclosporin A of ischemia/reperfusion-induced damage in isolated rat hearts, J. Mol. Cell. Cardiol. 25 (1993) 1461–1469.
[43] M.R. Duchen, O. McGuinness, L.A. Brown, M. Crompton, On the involvement of a cyclosporin A sensitive mitochondrial pore in myocardial reperfusion injury, Cardiovasc. Res. 27 (1993) 1790–1794.
[44] F. Di Lisa, R. Menabo, M. Canton, M. Barile, P. Bernardi, Opening of the mitochondrial permeability transition pore causes depletion of mitochondrial and cytosolic NAD^{+} and is a causative event in the death of myocytes in postischemic reperfusion of the heart, J. Biol. Chem. 276 (2001) 2571–2575.